

Interface optical phonons in spherical quantum-dot/quantum-well heterostructures

F. Comas and C. Trallero-Giner

Departamento de Física Teórica, Universidad de La Habana, Vedado 10400, Havana, Cuba

(Received 28 September 2002; published 3 March 2003)

Interface optical phonons are studied in the case of a spherical quantum-dot/quantum-well (QD/QW) heterostructure by applying a dielectric continuum approach. The prototypical case is a QD/QW of CdS/HgS in the form of spherical shell of HgS embedded on a spherical CdS QD, a kind of structure intensively investigated in the latter times. We also assume the QD/QW heterostructure surrounded by a host material which is modeled in the form of an infinite dielectric medium which does not participate of the polar optical vibrations. The possible interface phonon modes (CdS- and HgS-SO phonons), the corresponding frequencies and the electron-phonon interaction Hamiltonian are reported. A detailed discussion is made of the SO phonons fundamental characteristics and of the strength of the electron-phonon interaction.

DOI: 10.1103/PhysRevB.67.115301

PACS number(s): 63.22.+m, 71.38.-k

I. INTRODUCTION

In the framework of the dielectric continuum approach (DCA) polar optical vibrations of small size crystals have been theoretically investigated since a long time ago.¹ The quantum version of these vibrations are the internal LO and TO phonons, as well as the SO phonons associated to the crystal boundary surfaces. The latter type of phonons are due to the different dielectric constants at the interfaces and are also called *interface* optical phonons. Progress in the growth technology has made possible to fabricate small crystals in the nanometer scale (nanoparticles), where the three spatial dimensions are substantially reduced down to a quasi-zero-dimensional system. The so-called *quantum dots* (QD's) are semiconductor nanoparticles where the linear dimensions are comparable to (or even smaller than) the corresponding exciton Bohr radius. At the present level of technological sophistication QD's with relatively well defined and controllable size distributions are fabricated.²⁻⁵ The host material may be a silicate matrix, different organic compounds or a ferroelectric.⁶ The physical properties of QD's are usually studied by means of optical experiments, such as Raman spectroscopy, hole burning, luminescence, etc., actually allowing us to investigate the system at an almost individual level.⁷⁻¹⁰ Particularly, these experimental techniques permit us to detect the QD phonons¹¹ and study their properties.

By applying the DCA, polar optical phonons in QD's of the CdSe or CdS prototypes have been theoretically investigated assuming a spherical geometry and considering a non-vibrating host material as an infinite dielectric medium in which the QD is imbedded.^{12,13} The case of a QD with ellipsoidal shape was recently studied,^{14,15} while in all the above-mentioned works the electron-phonon interaction Hamiltonian was explicitly derived and its influence on Raman spectra line shapes was also analyzed. The question when the DCA will correctly describe the interface optical oscillations obviously is related to the QD linear dimensions L . An estimation can be made using the bulk phonon wavelength λ_p and requiring it to be smaller than L ($\lambda_p < L$). Actually, if $\lambda_p \geq L$, the mechanical boundary conditions should be included in the treatment, while from the point of view of the Raman selection rules,¹⁶ the purely DCA in general leads to

misleading results. In such a case a more more rigorous and complete approach should be employed in order to obtain a reliable description of optical phonon modes.¹⁷⁻¹⁹

In recent times QD's of CdSe and CdS, as well as QD heterostructures of the type CdS/HgS, the so-called quantum-dot/quantum-well (QD/QW) heterostructures, are being synthesized by means of colloidal solution chemistry.²⁰⁻²² These structures show rather interesting size-dependent optical properties (particularly concerning the fluorescence spectra) and appear to have promising perspectives for the development of electronic and optical devices. In the case of QD/QW heterostructures a few monolayers of HgS are epitaxially grown on a CdS core and, after that, the system may be capped or not with an additional layer of CdS.²¹ The whole system is imbedded in a host material, which usually is an organic compound. The bulk HgS has an energy gap ($E_g = 0.5$ eV) lower than the bulk CdS ($E_g = 2.5$ eV), and hence a true quantum-well heterostructure is created within the QD. Experimental evidence demonstrates the presence of highly confined carriers in the HgS layer.

The fundamental aim of the current work is to study the SO phonons by applying the DCA to the case of a prototypical spherical QD heterostructure, which is modelled as follows: a spherical core of material "1" (say, CdS) is capped with a spherically concentric layer of material "2" (say, HgS) and the whole structure is imbedded in a host material considered as an infinite dielectric medium which does not participate of the polar optical vibrations. Consistently applying the basic equations of the DCA we deduce the SO phonon frequencies for QD- and QW-type modes as a function of the radius ratio of the core sphere to the external shell cap. The physical nature of these SO phonon branches is interpreted and related to the QD/QW structure. We also make a detailed derivation of the electric potential as a function of the spatial coordinates for each of the possible SO phonon branches, thus allowing to deduce an explicit expression for the electron-phonon interaction Hamiltonian, whose physical features are discussed. Despite the simple character of the applied model, we actually obtain interesting properties of the SO phonons bearing a clear physical interpretation, which, as we will discuss in the text below, may be used to interpret Raman measurements and should provide direct

information about the geometric parameters characterizing the QD/QW heterostructures.

The paper is organized as follows. In Sec. II we present a brief summary of the fundamental equations of the DCA and apply them to our model system. Section III is devoted to the study of the SO phonon dispersion law, i.e., we describe the frequency branches as a function of the radius ratio of the heterostructure. In Sec. IV we derive the electric potential and the electron-phonon Hamiltonian. Finally, Sec. V presents a detailed discussion of the main results of the work.

II. GENERAL EQUATIONS

For the sake of clarity, let us briefly summarize the fundamental equations of the DCA for the description of the polar optical phonons. They are extensively discussed in the existing literature on the subject.^{1,12-15} The Born-Huang equations are

$$\ddot{\mathbf{w}} = -\omega_T^2 \mathbf{w} + \sqrt{(\varepsilon_0 - \varepsilon_\infty)/4\pi\omega_T} \mathbf{E} \quad (1)$$

and

$$\mathbf{P} = \sqrt{(\varepsilon_0 - \varepsilon_\infty)/4\pi\omega_T} \mathbf{w} + \frac{\varepsilon_\infty - 1}{4\pi} \mathbf{E}, \quad (2)$$

where $\mathbf{w} = \sqrt{\rho} \mathbf{u}$, \mathbf{u} represents the relative displacement between the ion pair (in units of length), ρ is the reduced mass density addressed to the ion pair of the vibrating medium. Other quantities are the electric field \mathbf{E} , the polarization field \mathbf{P} , the transversal limit bulk frequency ω_T , and the static (high frequency) dielectric constant ε_0 (ε_∞). Moreover, we assume the Lyddane-Sachs-Teller relation $\omega_L^2/\omega_T^2 = \varepsilon_0/\varepsilon_\infty$ with ω_L being the LO phonon frequency. Considering that the electric field satisfies quasistatic Maxwell equations, we must require the induction field $\mathbf{D} = \varepsilon(\omega)\mathbf{E} = \mathbf{E} + 4\pi\mathbf{P}$ to fulfil the equation $\nabla \cdot \mathbf{D} = 0$. If the relation $\mathbf{E} = -\nabla\varphi$ is assumed, we are led to

$$\varepsilon(\omega)\nabla^2\varphi = 0. \quad (3)$$

In all the above equations the harmonic time dependence of the form $f(t) \sim \exp(-i\omega t)$ is applied. Then, the frequency dependent dielectric function $\varepsilon(\omega)$ is easily derived and is given by the standard expression $\varepsilon(\omega) = \varepsilon_\infty(\omega^2 - \omega_L^2)/(\omega^2 - \omega_T^2)$. The SO phonons involve an electric potential satisfying the Laplace equation $\nabla^2\varphi = 0$, in which case $\varepsilon(\omega) \neq 0$. The potential φ should be continuous at the interface between two different media and also must fulfil the boundary condition

$$\varepsilon_1 \left[\frac{\partial\varphi_1}{\partial n} \right]_S = \varepsilon_2 \left[\frac{\partial\varphi_2}{\partial n} \right]_S, \quad (4)$$

i.e., continuity of the normal component of \mathbf{D} at the interface surface S . A complementary relation, which proves to be rather useful in what follows, reads

$$\nabla\varphi = \frac{\varepsilon_\infty\omega_L}{\varepsilon_\infty - \varepsilon(\omega)} \sqrt{\frac{4\pi\rho}{\varepsilon^*}} \mathbf{u}, \quad \frac{1}{\varepsilon^*} = \frac{1}{\varepsilon_\infty} - \frac{1}{\varepsilon_0}. \quad (5)$$

We need to solve Laplace equation for the electric potential φ in the whole space. The geometry of the studied system is the following: for $0 < r < a$ we have material “1” (a polar semiconductor such as CdS), for $a < r < b$ we have material “2” (a different polar semiconductor such as HgS), for $r > b$ we shall assume an infinite dielectric medium with a fixed dielectric constant ε_D . Using spherical coordinates (r, θ, ϕ) the potential is given by

$$\begin{aligned} \varphi_{lm}(r, \theta, \phi) &= A_{lm} Y_{lm}(\theta, \phi) \\ &\times \begin{cases} r^l, & r < a, \\ \frac{\beta_l - 1}{\gamma^{2l+1} - 1} r^l + \frac{\gamma^{2l+1} - \beta_l}{\gamma^{2l+1} - 1} \frac{a^{2l+1}}{r^{l+1}}, & a < r < b, \\ \beta_l \frac{a^{2l+1}}{r^{l+1}}, & r > b, \end{cases} \quad (6) \end{aligned}$$

where

$$\begin{aligned} \beta_l &= \frac{1}{2l+1} \{ [l+1 + l\varepsilon^{(1)}(\omega)/\varepsilon^{(2)}(\omega)] \gamma^{2l+1} \\ &\quad - l[\varepsilon^{(1)}(\omega)/\varepsilon^{(2)}(\omega) - 1] \}. \quad (7) \end{aligned}$$

In Eq. (6) the potential φ_{lm} obviously satisfies Laplace equation in the whole space, is already continuous at $r = a$ and $r = b$ and shows the correct asymptotic behavior $\varphi_{lm} \rightarrow 0$ for $r \rightarrow 0$ and $r \rightarrow \infty$. The fulfillment of boundary condition (4) at $r = a$ and $r = b$ has been also ensured conducting to the expression for β_l given by Eq. (7) and to the SO phonon dispersion relation [see Eq. (9) below]. The quantities $Y_{lm}(\theta, \phi)$ and A_{lm} are the Harmonic Spherical functions and the normalization constants, respectively. The dielectric functions $\varepsilon^{(1)}(\omega)$ and $\varepsilon^{(2)}(\omega)$ correspond to materials “1” and “2,” respectively, while, according to the general (dispersionless) DCA, are given by

$$\varepsilon^{(i)}(\omega) = \varepsilon_\infty^{(i)} \frac{\omega^2 - \omega_{iL}^2}{\omega^2 - \omega_{iT}^2} \quad \text{with } i = 1, 2, \quad (8)$$

where ω_{iL} and ω_{iT} are the bulk longitudinal and transversal polar optical phonons frequencies at the Γ point for each semiconductor material ($i = 1, 2$), while $\gamma = b/a$. For a complete determination of the potential φ_{lm} we have to determine the constants A_{lm} . This will be left to Sec. IV.

III. SO PHONONS DISPERSION RELATIONS

As we mentioned in the previous section the boundary conditions led to the SO phonons dispersion equation

$$\frac{\varepsilon^{(2)}(\omega)}{\varepsilon_D} = - \frac{[\gamma^{2l+1} - 1]\varepsilon^{(1)}(\omega) + [1 + \gamma^{2l+1}(l+1)/l]\varepsilon^{(2)}(\omega)}{[\gamma^{2l+1} - 1]\varepsilon^{(2)}(\omega) + [1 + \gamma^{2l+1}l/(l+1)]\varepsilon^{(1)}(\omega)}. \quad (9)$$

Equation (9) gives the SO phonon frequencies as a function of the parameter γ for different values of l ($l=1,2,\dots$), and may be considered the dispersion relations for this kind of phonon. As remarked before, we do not have here phonons in the usual sense and a phonon wave vector does not appear at all.¹¹ It is instructive to analyze two limiting cases of Eq. (9). (i) The limit $\gamma \rightarrow 1$. In this case we are led to

$$\frac{\varepsilon^{(1)}(\omega)}{\varepsilon_D} = - \frac{l+1}{l}. \quad (10)$$

This limit corresponds to a single sphere of radius a and material “1,” imbedded in a dielectric infinite medium. Equation (10) is in total coincidence with previous results^{1,12} as should be expected. (ii) The limit $\gamma \rightarrow \infty$. Notice that this limit may be achieved in two cases: (A) $a \rightarrow 0$ with a fixed value of b and (B) $b \rightarrow \infty$ with a fixed value of a . Equation (9) reduces to

$$\frac{\varepsilon^{(2)}(\omega)}{\varepsilon_D} = - \frac{l+1}{l} \frac{l\varepsilon^{(1)}(\omega) + (l+1)\varepsilon^{(2)}(\omega)}{(l+1)\varepsilon^{(2)}(\omega) + l\varepsilon^{(1)}(\omega)}. \quad (11)$$

The above relation involves a quadratic equation for $\varepsilon^{(2)}(\omega)$ and leads to two possible roots:

$$(A) \quad \frac{\varepsilon^{(2)}(\omega)}{\varepsilon_D} = - \frac{l+1}{l} \quad (B) \quad \frac{\varepsilon^{(1)}(\omega)}{\varepsilon^{(2)}(\omega)} = - \frac{l+1}{l}, \quad (12)$$

corresponding to the cases (A) and (B) as is explicitly indicated in Eq. (12). From the above analysis we see that, for each value of l , we have three possible SO phonon branches. Actually, case (A) in Eq. (12) defines a single frequency given by

$$x_A^{(\infty)} = \frac{l x_{2L} + (l+1) \varepsilon_D x_{2T} / \varepsilon_\infty^{(2)}}{l + (l+1) \varepsilon_D / \varepsilon_\infty^{(2)}} \quad (13)$$

which depends on ε_D , while case (B) in Eq. (12) defines two frequencies

$$x_{\pm B}^{(\infty)} = \frac{y \pm [y^2 - 4(1 + \alpha_l)(x_{1L} x_{2T} + \alpha_l x_{2L})]^{1/2}}{2(1 + \alpha_l)}, \quad (14)$$

where $y = x_{1L} + x_{2T} + \alpha_l(1 + x_{2L})$, $\alpha_l = (l+1)\varepsilon_\infty^{(2)}/l\varepsilon_\infty^{(1)}$, and $x = (\omega/\omega_{1T})^2$. In correspondence with this notation $x_{1L} = (\omega_{1L}/\omega_{1T})^2$, $x_{2L} = (\omega_{2L}/\omega_{1T})^2$, etc. The frequencies defined by Eq. (14) are independent of ε_D .

Considering the spatial symmetry of the QD/QW structure we must expect two classes of interface phonons. One of them should be related to a spherical QD embedded in certain host material and the other ones are connected to the two interfaces involved in the QW structure. Thus, this physical

analysis leads us to the prediction of three independent phonon branches for the structure under consideration. From the mathematical point of view the existence of three SO phonon branches can be directly demonstrated by realizing that Eq. (9) is a cubic equation in the x , which reads

$$x^3 - P_l x^2 + Q_l x - S_l = 0. \quad (15)$$

The coefficients in Eq. (15) are given in the Appendix A. The above equation has three different real solutions which can be classified according to the classical Cardano's (or Tartaglia's) formula as²³

$$x_1 = \frac{1}{3} P_l + 2 \left[-\frac{1}{27} \left(Q_l - \frac{1}{3} P_l^2 \right)^3 \right]^{1/3} \cos \Theta/3, \quad (16)$$

$$x_2 = \frac{1}{3} P_l + 2 \left[-\frac{1}{27} \left(Q_l - \frac{1}{3} P_l^2 \right)^3 \right]^{1/3} \cos(\Theta/3 + 2\pi/3), \quad (17)$$

$$x_3 = \frac{1}{3} P_l + 2 \left[-\frac{1}{27} \left(Q_l - \frac{1}{3} P_l^2 \right)^3 \right]^{1/3} \cos(\Theta/3 + 4\pi/3), \quad (18)$$

where

$$\Theta = \cos^{-1} \left\{ \frac{S_l + 2P_l^3/27 - P_l Q_l/3}{[-4(Q_l - P_l^2/3)^3/27]^{1/2}} \right\}. \quad (19)$$

The obtained solutions describe the three possible phonon branches (for each value of l) already mentioned in the text above. It can be proved that the root x_3 [Eq. (18)] for $\gamma \rightarrow \infty$ leads to the asymptotic value $x_A^{(\infty)}$ [Eq. (13)]. In the same limit the root x_1 [Eq. (16)] has $x_{+B}^{(\infty)}$ [Eq. (14) with the upper sign] as asymptotic value, while x_2 [Eq. (17)] has its asymptotic value defined by the same equation with the lower sign ($x_{-B}^{(\infty)}$). The identification of the frequency asymptotes (for $\gamma \rightarrow \infty$) corresponding to the three different roots gives us a certain physical insight into the nature of these vibration modes. A more detailed discussion is left to Sec. V.

IV. ELECTRON-PHONON HAMILTONIAN

In order to introduce a quantum description of the SO phonons we define the annihilation and creation operators \hat{a}_{lm} and \hat{a}_{lm}^\dagger obeying bosonic commutation relations $[\hat{a}_{lm}, \hat{a}_{l'm'}^\dagger] = \delta_{ll'} \delta_{mm'}$, etc. Then, the displacement vector \mathbf{u} is transformed into the operator $\hat{\mathbf{u}}$ by means of

$$\hat{\mathbf{u}}_{lm} = \begin{cases} u_0 \nabla(r^l Y_{lm}) \hat{a}_{lm}, & r < a, \\ u_{10} \nabla \left[\left((\beta_l - 1) r^l + (\gamma^{2l+1} - \beta_l) \frac{a^{2l+1}}{r^{l+1}} \right) Y_{lm} \right] \hat{a}_{lm}, & a < r < b. \end{cases} \quad (20)$$

The potential operator $\hat{\phi}_{lm}$ can be obtained from Eq. (20) with the help of Eq. (5). The continuity of this operator at $r=a$ leads to

$$u_{10} = \left(\frac{\varepsilon_{\infty}^{(1)} \omega_{1L}}{\varepsilon_{\infty}^{(2)} \omega_{2L}} \right) \left(\frac{\varepsilon_{\infty}^{(2)} - \varepsilon^{(2)}(\omega)}{\varepsilon_{\infty}^{(1)} - \varepsilon^{(2)}(\omega)} \right) \sqrt{\frac{\varepsilon_2^* \rho_1}{\varepsilon_1^* \rho_2}} u_0 = \sqrt{C_l(\omega)} u_0. \quad (21)$$

The potential operator for $r < a$ and $a < r < b$ is then given by

$$\hat{\phi}_{lm} = A_l(\omega) Y_{lm} \begin{cases} r^l \hat{a}_{lm}, & r < a, \\ \left[\frac{\beta_l - 1}{\gamma^{2l+1} - 1} r^l + \frac{\gamma^{2l+1} - \beta_l}{\gamma^{2l+1} - 1} \frac{a^{2l+1}}{r^{l+1}} \right] \hat{a}_{lm}, & a < r < b, \\ a < r < b, \end{cases} \quad (22)$$

where

$$A_l(\omega) = \frac{\varepsilon_{\infty}^{(1)} \omega_{1L}}{\varepsilon_{\infty}^{(1)} - \varepsilon^{(1)}(\omega)} \sqrt{\frac{4\pi\rho_1}{\varepsilon_1^*}} u_0. \quad (23)$$

Now we shall determine the constant u_0 . The classical kinetic energy due to the vibrations is given by

$$W_{kin} = \frac{1}{2} \rho_1 \omega^2 \int_{V_1} \mathbf{u}^2 dV + \frac{1}{2} \rho_2 \omega^2 \int_{V_2} \mathbf{u}^2 dV, \quad (24)$$

where V_1 (V_2) is the volume of the region $r < a$ ($a < r < b$). The energy W_{kin} is transformed into an operator by means of $\mathbf{u} \rightarrow \hat{\mathbf{u}}$, but it must be realized that the operator defined in Eq. (20) is not Hermitian. For that reason the correct transformation is $\mathbf{u}^2 \rightarrow (\hat{\mathbf{u}}^\dagger \cdot \hat{\mathbf{u}} + \hat{\mathbf{u}} \cdot \hat{\mathbf{u}}^\dagger)/2$. After a simple manipulation of this result, we obtain

$$\hat{H}_{ph}^{(lm)} = \frac{1}{2} u_0^2 \omega^2 M_l \left(\hat{a}_{lm}^\dagger \hat{a}_{lm} + \frac{1}{2} \right), \quad (25)$$

where

$$M_l = \rho_1 \int_{V_1} \nabla \xi_1^* \cdot \nabla \xi_1 dV + \rho_2 C_l(\omega) \int_{V_2} \nabla \xi_2^* \cdot \nabla \xi_2 dV. \quad (26)$$

In Eq. (25) we use the notation $\hat{H}_{ph}^{(lm)}$ for the SO phonon Hamiltonian operator. Other functions appearing in Eq. (26) are

$$\xi_1 = r^l Y_{lm}, \quad \xi_2 = \left[\frac{\beta_l - 1}{\gamma^{2l+1} - 1} r^l + \frac{\gamma^{2l+1} - \beta_l}{\gamma^{2l+1} - 1} \frac{a^{2l+1}}{r^{l+1}} \right] Y_{lm}. \quad (27)$$

The volume integrals in Eq. (26) can be analytically performed. This calculation is given in Appendix B. We require that $\hat{H}_{ph}^{(lm)}$ should be expressed in its standard harmonic form $\hat{H}_{ph}^{(lm)} = \hbar \omega (\hat{a}_{lm}^\dagger \hat{a}_{lm} + 1/2)$. Then, the constant u_0 is determined by

$$u_0^2 = \frac{2\hbar}{\omega M_l}, \quad (28)$$

where M_l is explicitly given in Eq. (B7). The above procedure permits to evaluate the constants A_{lm} present in Eq. (6) [also in Eqs. (22) and (23)]:

$$A_l(\omega) = \frac{\varepsilon_{\infty}^{(1)} \omega_{1L}}{\varepsilon_{\infty}^{(1)} - \varepsilon^{(1)}(\omega)} \left[\frac{8\pi\hbar\rho_1}{\varepsilon_1^* \omega M_l} \right]^{1/2}. \quad (29)$$

Notice that A_{lm} actually depends just on l . We have thus obtained an explicit analytic expression for the potential operator $\hat{\phi}_{lm}$:

$$\hat{\phi}_{lm} = \frac{A_l(\omega)}{2} \begin{cases} Y_{lm} r^l \hat{a}_{lm} + \text{H.c.}, & r < a, \\ Y_{lm} \left[\frac{\beta_l - 1}{\gamma^{2l+1} - 1} r^l + \frac{\gamma^{2l+1} - \beta_l}{\gamma^{2l+1} - 1} \frac{a^{2l+1}}{r^{l+1}} \right] \hat{a}_{lm} + \text{H.c.}, & a < r < b, \\ Y_{lm} \beta_l \frac{a^{2l+1}}{r^{l+1}} \hat{a}_{lm} + \text{H.c.}, & r > b, \end{cases} \quad (30)$$

where ‘‘H.c.’’ stands for ‘‘Hermitian conjugate.’’ Obviously, the operator $\hat{\phi}_{lm}$ in Eq. (30) is Hermitian. Finally, the electron-phonon interaction Hamiltonian is given by

$$\hat{H}_{e-ph}^{(lm)} = -e \hat{\phi}_{lm}(r, \theta, \phi). \quad (31)$$

V. DISCUSSION OF THE OBTAINED RESULTS

Let us make a detailed physical discussion of the main results obtained in the foregoing sections. For the numerical

computations we considered that material ‘‘1’’ is CdS and material ‘‘2’’ is HgS. The values of the corresponding physical parameters are given in Table I. Concerning the host material where the QD/QW is imbedded we used essentially the dielectric constant $\varepsilon_D = 4.64$ (except a particular case where the value $\varepsilon_D = 2$ was applied).

In Figs. 1 and 2 we analyze the dispersion relation, i.e., the frequency dependence on the parameter $\gamma = b/a$ for the three types of vibration modes obtained and for various val-

TABLE I. Values of the semiconductor physical parameters.

Material	ϵ_∞	ϵ_0	$\omega_T(cm^{-1})$	$\omega_L(cm^{-1})$
CdS	5.5	9.1	233	300
HgS	11.36	18.2	197.5	250

ues of l . We are using the notation $x = (\omega/\omega_{1T})^2$ as described in the text above. Thus, x denotes the squared frequencies in units of ω_{1T} . The squared frequencies of the three vibration modes found in our calculations are given by the variables x_i ($i=1,2,3$), which are the roots of Eq. (15), and were explicitly reported in Eqs. (16)–(18) as a function of γ and l . Figure 1(a) describes the root x_1 for three values of l ($l=1,2,3$). The dotted lines correspond to the strictly spherical QD of CdS imbedded in a dielectric medium of dielectric constant $\epsilon_D=4.64$.^{1,12} The dashed lines give the corresponding asymptotes ($\gamma \rightarrow \infty$) according to Eq. (14), i.e., $x_{+B}^{(\infty)}$. This asymptote [case (B)] implies the limit when $b \rightarrow \infty$ and a is fixed, i.e., a CdS sphere of radius a imbedded in an infinite semiconductor medium made of HgS. The curves increase for larger values of γ (and also of l), while for $\gamma=1$ reproduce the case of a sphere of CdS imbedded in a dielectric infinite medium. The root x_1 corresponds to the QD-SO phonon modes, i.e., to the interface phonons of a spherical CdS dot imbedded in a certain host material (HgS+ infinite dielectric medium) with a certain effective dielectric constant. The influence of this “effective host” dielectric constant on the vibration frequencies is determined by the Eq. (16) with an asymptotic behavior ruled by $x_{+B}^{(\infty)}$. In order to get a more clear insight into the dependence of the Cd-SO phonon modes on the host dielectric constant, in Fig. 1(b) we present

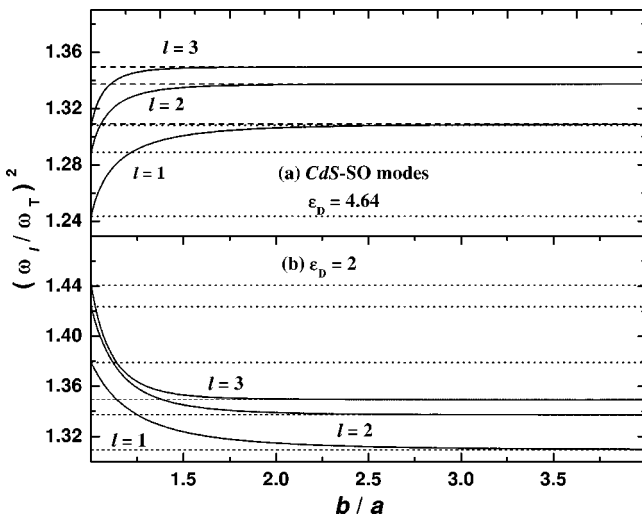


FIG. 1. Squared interface optical phonon frequencies of a QD/QW $(\omega_l/\omega_{1T})^2$ as a function of $\gamma=b/a$ for three values of l : $l=1,2,3$. These curves correspond to the CdS-SO phonon branch given by the root x_1 as explained in the text. The dotted lines represent the strictly spherical QD case (size independent) and the dashed lines give the asymptotes $x_{+B}^{(\infty)}$ [see Eq. (14)] for $\gamma \rightarrow \infty$. (a) Host dielectric constant $\epsilon_D=4.64$. (b) $\epsilon_D=2$. In this case the asymptotes are below the lines of the strictly spherical QD.

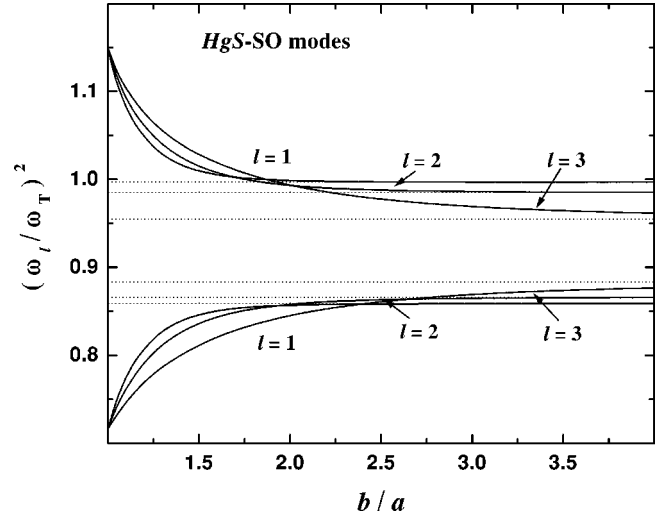


FIG. 2. Squared frequencies $(\omega_l/\omega_{1T})^2$, of the HgS-SO phonon modes as a function of $\gamma=b/a$ for $l=1,2,3$. The upper branches correspond to the SO phonon modes given by the root x_3 [see Eq. (18)] while the lower branches to the modes x_2 [see Eq. (17)] as explained in the text. Dotted lines represent the $x_A^{(\infty)}$ and $x_B^{(\infty)}$ asymptotes of the x_3 and x_2 functions, respectively. In the calculation the value of $\epsilon_D=4.64$ was used.

the same case (root x_1) but now we have taken $\epsilon_D=2$. As can be seen, in this case the frequencies decrease for larger values of γ . The point is that in this case the lines for the strictly spherical case (and for each l) are shifted upwards due to the smaller value of ϵ_D , while the asymptotes do not depend on ϵ_D . Hence, the slope of these curves critically depends on the value of ϵ_D . We should remark that host materials with a relatively wide range in the values of ϵ_D have been reported in the literature (see, for instance Ref. 6).

Figure 2 displays the roots x_3 (upper branches) and x_2 (lower branches) for the firsts three values of l . Again the dotted lines represent the asymptotes as given by $x_A^{(\infty)}(l)$ [Eq. (13)] for the upper branches and $x_B^{(\infty)}(l)$ [Eq. (14)] for the lower branches. The curves may be closely related to the case of interface optical phonons in a typical quantum well heterostructure, and, therefore, should be associated with a kind of interface LO phonons of the spherical HgS QW sandwiched between a spherical CdS QD and a host dielectric medium. Let us remark that in Fig. 2 the limit $\gamma=1$ was also included, but this limit has no physical meaning. Actually, the corresponding vibration modes associated with these frequencies shall be present whenever the layer of semiconductor “2” (i.e., HgS) has a finite thickness, i.e., $b-a \neq 0$. We have also analyzed the Hg-SO branches for different values of the dielectric constant ϵ_D , but the general trends of the curves do not change essentially (just their separation is uniformly changed for the upper or lower branches).

In order to get a deeper physical insight into the nature of the vibration modes, it is interesting to study the strength of the electron-phonon interaction for the different possible modes. In that connection, we analyzed the radial part of the electrostatic potential $\Phi_l(r)$, where we assume $\varphi_{lm}(r, \theta, \phi) = \Phi_l(r)Y_{lm}(\theta, \phi)$. Figure 3(a) shows $\Phi_l(r)$ as a function of the dimensionless radius r/a for the CdS-SO phonon

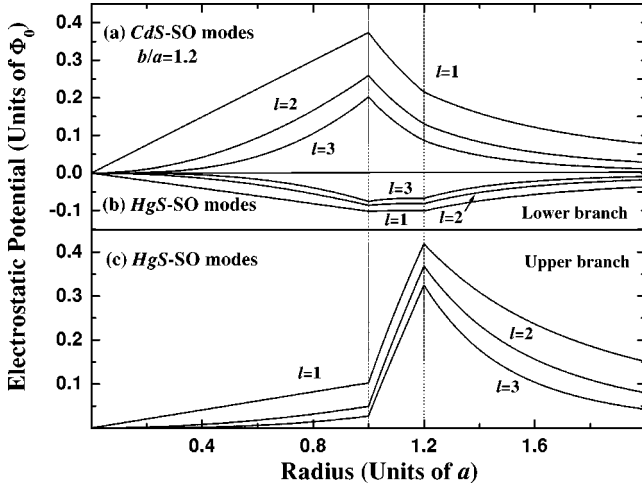


FIG. 3. Radial part of the electrostatic potential $\Phi_l(r)$, in units of Φ_0 , as a function of r/a for $l=1, 2$, and 3 . (a) CdS-interface phonon modes according to the x_1 root. (b) HgS-SO phonon modes given by the root x_2 (lower branches of Fig. 2). (c) HgS-SO phonons for the modes x_3 (upper branches of Fig. 2). We fixed $\gamma = 1.2$ and $\epsilon_D = 4.64$.

branches with $l=1, 2$, and 3 [shown in Fig. 1(a)]. We have fixed $\gamma = b/a = 1.2$, the value of $\epsilon_D = 4.64$ was applied, and the potential has been measured in units of Φ_0 , where

$$\Phi_0 = \sqrt{\frac{8\pi\hbar\omega_{1L}}{a\epsilon_1^*}}. \quad (32)$$

As evidently seen in the figure, the strength of the interaction is sharply peaked at $r=a$ indicating that these modes are strongly localized at the interface between materials “1” and “2.” The other interface is not essentially contributing to the interaction. In Fig. 3(b) the radial part of the electrostatic potential for the HgS-SO modes is shown and the root x_2 (lower branch of Fig. 2) is selected for the same values of γ and ϵ_D . It is obvious from the figure that in the present case the interaction strength is simultaneously peaked at both interfaces and that the absolute value of the potential is slightly lower. Moreover, the interaction strength is extended within the whole layer of material “2” resembling the typical QW interface phonons. Figure 3(c) presents $\Phi_l(r)$ for HgS interface phonons, but now the root x_3 was used (upper branch of Fig. 2). Figure 3(c) describes the same kind of dependence as in Fig. 3(a), but in this case the interaction strength is concentrated in the other interface at $r=b$, while the interface at $r=a$ practically does not provide an essential contribution. Thus, the two vibration modes x_1 and x_3 involve SO phonons in a situation where the system effectively behaves as if just a single interface would be present. They resemble the cases of single spheres with radius $r=a$ or $r=b$, respectively, while the medium outside ($r=a$) or inside ($r=b$) the spheres could be identified as a certain composite. The frequency asymptotes analyzed in Sec. III are just extreme situations for $\gamma \rightarrow \infty$. Actually, the asymptote related to the frequency x_1 implies a single sphere of radius a in an infinite semiconductor medium when $b \rightarrow \infty$. The asymptote related

to the frequency x_3 corresponds to a single sphere of radius b when $a=0$ and the external medium is an infinite dielectric continuum.

In different works on this subject it has been claimed that SO phonons do not involve a very strong interaction with the carriers. From our analysis it appears that this interaction may be certainly more important, particularly concerning the type of QD/QW we are considering. A more detailed analysis of the electron-phonon interaction shall be left for a future paper.

A direct application of the above exposed results is related to the determination of the QD/QW size, i.e., the values of the radii a and b of the contributing semiconductor materials. This is an important issue for the growth control of the QD structures. Raman measurements applied to these novel heterostructures should provide information about phonon modes and electron-phonon interaction as a function of the QD/QW radii. Due to the spherical symmetry, first order LO Raman scattering is allowed for phonons with $l=0$ angular momentum.^{17,18} Nevertheless, a clear and well defined shoulder at the left side of the main LO peak was observed in the Raman spectra of QD's (see, for example, Ref. 10 and references therein). The presence of this shoulder is usually associated to the SO-phonon contribution considering the breakdown of the selection rule ($l \neq 0$). Hence, Raman spectroscopy applied to QD/QW structures shall be a powerful technique for the detection of the corresponding shoulders located at well defined frequencies and related to the QD-SO and QW-SO phonon modes according to the results presented in Figs. 1 and 2. We may finally conclude that the present theoretical study of SO phonons together with the data from Raman spectra should provide a relatively precise determination of the QD/QW geometry, especially concerning the growth parameter $\gamma = b/a$.

APPENDIX A:

Coefficients P_l , Q_l , and S_l in the Eq. (15) are given by

$$R_l P_l = [1 + 2x_{2L} + \delta(x_{1L} + 2x_{2T})](\gamma^{2l+1} - 1) + (x_{2T} + x_{2L} + x_{1L})F_l + (1 + x_{2T} + x_{2L})G_l, \quad (A1)$$

$$R_l Q_l = [x_{2L}^2 + 2x_{2L} + \delta(2x_{2T}x_{1L} + x_{2T}^2)](\gamma^{2l+1} - 1) + (x_{2T} + x_{2L}x_{2T}x_{2L})G_l + (x_{2L}x_{2T} + x_{1L}x_{2T} + x_{1L}x_{2L})F_l, \quad (A2)$$

$$R_l S_l = (x_{2L}^2 + \delta x_{1L}x_{2T}^2)(\gamma^{2l+1} - 1) + x_{1L}x_{2L}x_{2T}F_l + x_{2T}x_{2L}G_l, \quad (A3)$$

where

$$R_l = F_l + G_l + (1 + \delta)(\gamma^{2l+1} - 1), \quad (A4)$$

$$F_l = \frac{\varepsilon_\infty^{(1)}}{\varepsilon_\infty^{(2)}} \left[1 + \frac{l}{l+1} \gamma^{2l+1} \right], \quad G_l = \frac{\varepsilon_D}{\varepsilon_\infty^{(2)}} \left[1 + \frac{l+1}{l} \gamma^{2l+1} \right], \quad (\text{A5})$$

and $\delta = \varepsilon_\infty^{(1)} \varepsilon_D / (\varepsilon_\infty^{(2)})^2$. The discriminant of the cubic equation (15) can be written as

$$\Delta_l = \frac{1}{4} \left[\frac{1}{3} P_l Q_l - \frac{2}{27} P_l^3 - S_l \right]^2 + \frac{1}{27} \left[Q_l - \frac{1}{3} P_l \right]^3 \quad (\text{A6})$$

and, in our case, is a negative quantity ($\Delta_l < 0$).

APPENDIX B:

Let us make the explicit calculation of M_l defined in Eq. (26). In the first place, we notice that

$$\nabla \xi_i \cdot \nabla \xi_i^* = \nabla \cdot (\xi_i \nabla \xi_i^*) - \xi_i \nabla^2 \xi_i^* = \nabla \cdot (\xi_i \nabla \xi_i^*) \quad (\text{B1})$$

because $\nabla^2 \xi_i^* = 0$ in each of the considered regions [ξ_i for $i=1,2$ are defined in Eq. (27)]. Then, both volume integrals present in Eq. (26) may be transformed into surface integrals of the form

$$I_i = \int_S \xi_i \nabla \xi_i^* \cdot N dS. \quad (\text{B2})$$

In Eq. (B2) N is the unit radial vector, $d\Omega$ is the element of solid angle, while N is a unit vector normal to the surface S enclosing the volume V . For $i=1$ we have

$$I_1 = \int_{S_a} \xi_1 \nabla \xi_1^* \cdot N r^2 d\Omega = l a^{2l+1}. \quad (\text{B3})$$

In Eq. (B3) N is the unit radial vector and S_a is the spherical surface of radius a . We used the normalization condition of the functions Y_{lm} , namely, $\int Y_{lm}^* Y_{lm} d\Omega = 1$. For $i=2$ the volume V_2 is enclosed between the spherical surfaces S_a and S_b . Then

$$I_2 = \int_S \xi_2 \nabla \xi_2^* \cdot N r^2 d\Omega = I_2' - I_2'', \quad (\text{B4})$$

where I_2' (I_2'') involves the spherical surface S_b (S_a). We are choosing N in the outward direction to the spherical surfaces. It is not difficult to find that

$$I_2' = l \beta_l [\beta_l + \varepsilon^{(1)}(\omega) / \varepsilon^{(2)}(\omega) - 1] \left(\frac{a}{\gamma} \right)^{2l+1}, \quad (\text{B5})$$

$$I_2'' = l a^{2l+1} \varepsilon^{(1)}(\omega) / \varepsilon^{(2)}(\omega). \quad (\text{B6})$$

Substituting the latter expressions for $I_{1,2}$ in Eq. (26), and after straightforward simplifications, we are led to

$$M_l = l \rho_1 a^{2l+1} \left\{ 1 + \frac{\varepsilon_1^*}{\varepsilon_2^*} \left[\frac{\omega_{1L} \varepsilon^{(2)}(\omega)}{\omega_{2L} \varepsilon^{(1)}(\omega)} \right]^2 \right. \\ \left. \times \left[\frac{\beta_l [\beta_l - 1 + \varepsilon^{(1)}(\omega) / \varepsilon^{(2)}(\omega)]}{\gamma^{2l+1}} - \frac{\varepsilon^{(1)}(\omega)}{\varepsilon^{(2)}(\omega)} \right] \right\}. \quad (\text{B7})$$

- ¹R. Ruppin and R. Englman, Rep. Prog. Phys. **33**, 149 (1970), and references therein.
- ²A.I. Ekimov, J. Lumin. **70**, 1 (1996).
- ³D. Bertram, O.I. Micic, and A.J. Nozik, Phys. Rev. B **57**, 4265 (1998).
- ⁴C.B. Murray, C.R. Kagan, and M.G. Bawendi, Science **270**, 1335 (1995).
- ⁵A.A. Guzelian, U. Banin, A.V. Kadanovich, X. Peng, and A.P. Alivisatos, Appl. Phys. Lett. **69**, 1432 (1996).
- ⁶J. Zhou, L. Li, Z. Gui, S. Buddhudu, and Y. Zhou, Appl. Phys. Lett. **76**, 1540 (2000).
- ⁷M.I. Vsilevskiy, A.G. Rolo, and M.J.M. Gomes, Solid State Commun. **89**, 587 (1994).
- ⁸A.M. de Paula, L.C. Barbosa, C.H.B. Cruz, O.L. Alves, J.A. Sanjurjo, and C.L. Cesar, Appl. Phys. Lett. **69**, 357 (1996).
- ⁹Yu.A. Pusep, G. Zanelatto, S.W. da Silva, J.C. Galzerani, P.P. González-Borrero, A.I. Toropov, and P. Basmaji, Phys. Rev. B **58**, R1770 (1998).
- ¹⁰C. Trallero-Giner, A. Debernardi, M. Cardona, E. Menéndez-Proupin, and A.I. Ekimov, Phys. Rev. B **57**, 4664 (1998).
- ¹¹In the case of nanoparticles the phonon concept is not quite appropriate. The system resembles a molecule and some authors prefer to use the word *vibron* instead of *phonon*.

- ¹²M.C. Klein, F. Hache, D. Ricard, and C. Flytzanis, Phys. Rev. B **42**, 11 123 (1990).
- ¹³S. Nomura and T. Kobayashi, Phys. Rev. B **45**, 1305 (1992).
- ¹⁴F. Comas, C. Trallero-Giner, N. Studart, and G.E. Marques, Phys. Rev. B **65**, 073303 (2002).
- ¹⁵F. Comas, C. Trallero-Giner, N. Studart, and G.E. Marques, J. Phys.: Condens. Matter **14**, 6469 (2002).
- ¹⁶C. Trallero-Giner, F. García-Moliner, V.R. Velasco, and M. Cardona, Phys. Rev. B **45**, 11 944 (1992).
- ¹⁷E. Roca, C. Trallero-Giner, and M. Cardona, Phys. Rev. B **49**, 13 704 (1994).
- ¹⁸M.P. Chamberlain, C. Trallero-Giner, and M. Cardona, Phys. Rev. B **51**, 1680 (1995).
- ¹⁹R. Rodríguez-Suárez, E. Menéndez-Proupin, and C. Trallero-Giner, Phys. Rev. B **62**, 11 006 (2000).
- ²⁰A. Mews, A. Eychmüller, M. Giersig, D. Schooss, and J. Weller, J. Phys. Chem. **98**, 934 (1994).
- ²¹A. Mews, A.V. Kadavanich, U. Banin, and A.P. Alivisatos, Phys. Rev. B **53**, R13 242 (1996).
- ²²F. Koberling, A. Mews, and T. Basché, Phys. Rev. B **60**, 1921 (1999).
- ²³G. A. Korn and T. M. Korn, *Mathematical Handbook* (McGraw-Hill, New York, 1968).